



Palladium and silk fibroin-containing magnetic nano-biocomposite: a highly efficient heterogeneous nanocatalyst in Heck coupling reactions

Ahmad Nouri Parouch¹ · Nadiya Koukabi¹ · Elham Abdous¹ · Seyed Amin Shobeiri¹

Received: 8 January 2021 / Accepted: 5 April 2021

© The Author(s), under exclusive licence to Springer Nature B.V. 2021

Abstract

Supported metal catalysts, for instance, palladium, are one of the foundations of chemical reactions, especially in C–C bond formation. The present study reports preparation of a magnetically separable palladium-supported nano-biocomposite with a low cost and easy immobilization technique. Fibroin, a natural biodegradable polymer, was used through an in situ method to cover the Fe₃O₄ nanoparticles to make a nano-biocomposite followed by anchoring palladium on the fibroin surface. The morphology and the structure of palladium-supported nano-biocomposite Fe₃O₄@fibroin-Pd were characterized by FT-IR, XRD, TGA, SEM, EDX, and TEM techniques. Consequently, the nanocatalyst activity was evaluated in the Heck coupling reactions. Only a very small amount of the nanocatalyst was employed in the reaction, and it showed excellent catalytic activity; in most cases more than 90% efficiency. The significant advantages of employing this nanocatalyst include high catalytic activity, short reaction times, easy separation of the nanocatalyst with an external magnet and great reusability. The results demonstrated that the used nanocatalysts were very active for four consecutive reaction rounds.

Keywords Biopolymer-supported Pd · Silk fibroin · Nano-biocomposite · Nanocatalyst · Heck coupling reaction

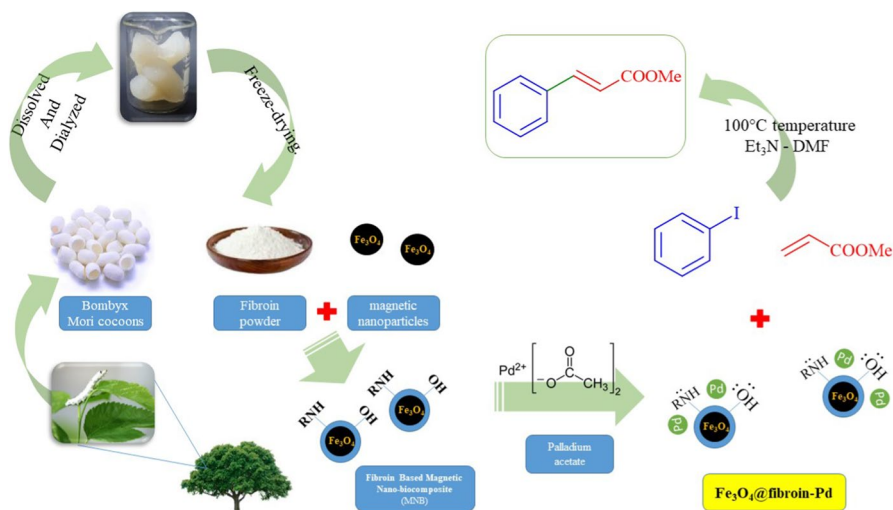
Introduction

In recent years, nanotechnology is gaining more attention to the utilization of natural sources like agro wastes [1], biological sources [2], and biopolymers for the preparation of nanoparticles [3]. There is a growing tendency for using biodegradable

✉ Nadiya Koukabi
n.koukabi@semnan.ac.ir

¹ Department of Chemistry, Semnan University, 35131-19111 Semnan, Iran

polymers in numerous fields such as drug delivery systems [4], medical load-bearing applications [5], commodity plastics [6], electronics [7], anticancer activities [8]. Using biodegradable materials results in construction of environmentally friendly products which is an important principle of green chemistry. The first steps toward synthesizing a green catalyst are designing and preparing a combination of biodegradable materials, namely biopolymers, with suitable materials to reach a biocomposite. Different biocomposites were synthesized using various biopolymers including proteins [9] and polysaccharides [10]. Besides, Fe_3O_4 nanoparticles (NPs) were used in preparation of magnetically separable heterogeneous catalysts, and different organic and inorganic shells were employed to produce core-shell nanostructures [11, 12]. The necessity to develop new strategies for coating the Fe_3O_4 NPs is barricade aggregation and air oxidation to increase stabilization and decreased vulnerability during catalytic applications [13]. Coating Fe_3O_4 NPs with polymers which have multiple functional groups allows us for further surface modifications with various catalytic agents for extensive catalytic applications [14]. Between the materials which can be used as a shell, fibroin is a great candidate because of high biocompatibility, biodegradability, stability, low costs, simple surface functionalization, and low toxicity [15, 16]. Therefore, fibroin offers a good opportunity in manufacturing and developing green and durable catalysts. Bombyx mori silk is an amphiphilic fibrous protein, mainly composed of fibroin and sericin as the core and coating layer, respectively [17]. Sericin is a protein with a molecular weight that varies from 10–20 to 310–400 kDa [18]. Also, fibroin is a linear polypeptide with 5263 amino acids residues composed of glycine, alanine, serine, tyrosine, valine, and only 4.7% of the other 15 amino acid types [19]. Although there are various reports about utilizing silk fibroin in different fields including, drug delivery [20], biomaterial [21], enzyme immobilization [22], tissue regenerations [23], and biomedical [24] applications, a few reports are related to its catalytic applications. Importantly, fibroin has functional groups such as carbonyl, amine, and hydroxyl groups on its surface. These functional groups can be used for surface modification to expand catalytic applications. A few papers investigated fibrous silk fibroin catalytic application as a support for nanoparticles of palladium [25], iron [26], and gold [27]. Unfortunately, two unavoidable problems are related to using bulky fibroin as catalyst support. Firstly, difficulty in separating the bulky fibroin from the reaction mixture and products. Secondly, bulky silk fibroin provides much less surface area and active sites in comparison with nanoparticles. The present study is a continuation of our previous studies toward developing new eco-friendly heterogeneous catalysts [28, 29] and offered a facile method to make Fe_3O_4 @fibroin-Pd then assessed in the Heck reaction. For this purpose, the first step was to cover the Fe_3O_4 NPs using purified fibroin powder for making a magnetic nano-biocomposite. In the second step, the fibroin-palladium complex formed through a green procedure. With the novel Fe_3O_4 @fibroin-Pd nanocatalyst in hand, Heck reaction was carried out to investigate its catalytic capability comprising activity and reusability (Scheme 1). Besides, parameters like amount of the nanocatalyst, solvent, reaction time, temperature, and base system were also investigated. Considering the importance of palladium in organic syntheses, this novel and unique nanocatalyst would gain wide attention.



Scheme 1 Procedure for preparation and application of Fe_3O_4 @fibroin-Pd

Experimental

Materials and methods

All chemicals were bought from Merck and Sigma-Aldrich and were employed without any purification. Bombyx mori cocoons were bought from Rasht, Iran. Iron (II) chloride tetrahydrate ($\text{FeCl}_2 \cdot 4\text{H}_2\text{O}$), iron (III) chloride hexahydrate ($\text{FeCl}_3 \cdot 6\text{H}_2\text{O}$), ammonium hydroxide (NH_4OH), sodium carbonate (Na_2CO_3), calcium chloride (CaCl_2), iodobenzene, methyl acrylate, butyl acrylate, triethylamine (Et_3N), dimethylformamide (DMF), aryl halides, ethyl acetate, magnesium sulfate (MgSO_4), and palladium acetate ($\text{Pd}(\text{OAc})_2$). Dialysis tubing cellulose membrane (cut-off = 14,000) was bought from Sigma-Aldrich.

SEM–EDX analysis was accomplished using MIRA3 TESCAN-XMU digital scanning microscope. TEM images were collected using a transmission electron microscope (TEM; Philips EM 208S-100 kV). X-ray diffraction (XRD) analysis was done on a Siemens D5000 (Siemens AG, Munich, Germany) using Cu-K α radiation of wavelength 1.54 Å. The thermogravimetric analysis (TGA) was performed using a Du Pont 2000 thermal analysis apparatus heated from 25 to 1000 °C at ramp 10 °C/min under air atmosphere. The FT-IR spectra were recorded by a Shimadzu 8400 s spectrometer using KBr pressed powder disks. The amount of palladium in the catalyst was measured with an Agilent model 240 AA Shimadzu (USA) flame atomic adsorption spectrometer. The NMR spectra obtained using a Bruker Avance 400 MHz instruments (^1H -NMR 400 MHz and ^{13}C -NMR 125 MHz) in pure dimethyl sulfoxide.

Fibroin preparation

Fibroin was purified and degummed according to previous reports [30]. To remove the sericin proteins, small slices of *Bombyx mori* cocoons boiled for 1 h in an aqueous solution of Na_2CO_3 5% (w/v) and then it was filtered through a filter paper followed by washing with hot water and drying overnight. The molecular weight of pure fibroin is around 95 kDa for the Na_2CO_3 -degumming *Bombyx mori* cocoons [31]. The extracted fibrous fibroin was added to a mixture of deionized water, calcium chloride, and ethanol with the mole ratio of 8:1:2 and kept at 90 °C to completely dissolved. The fibroin solution was dialyzed with a dialysis tube against deionized water for 3 days, and fibroin powder could be prepared by the freeze-drying technique.

Synthesis of magnetic nano-biocomposite

The magnetic nano-biocomposite (MNB) was synthesized through an in situ reaction according to the literature with some modification [32]. $\text{FeCl}_2 \cdot 4\text{H}_2\text{O}$ (1.789 g) and $\text{FeCl}_3 \cdot 6\text{H}_2\text{O}$ (4.865 g) were dissolved in 90 mL of distilled water followed by sonication until complete disappearance of solid particles. To this mixture under continuous stirring, 10 mL of the 10 wt% fibroin and then NH_4OH (10 mL) solution were added. Upon the formation of a black suspension, it was refluxed at 100 °C for 6 h under a nitrogen atmosphere and continuous stirring. Finally, MNB was isolated from the reaction mixture by an external magnet followed by washing with distilled water several times and then drying in the air.

Preparation of Fe_3O_4 @fibroin-Pd

The Fe_3O_4 @fibroin-Pd was prepared according to a green pathway without using organic solvents. At first, MNB (0.3 g) was added in distilled water (6 mL) and sonicated for 30 min. In the following, 6 mL palladium acetate solution (0.05 g $\text{Pd}(\text{OAc})_2$ in 6 mL water) was added to the above mixture. Finally, the last mixture was refluxed at 100 °C for 24 h under an N_2 atmosphere with constant stirring. After magnetically separating and washing with distilled water, Fe_3O_4 @fibroin-Pd nanocatalyst was obtained.

Results and discussion

Catalyst characterization

SEM/EDX

The surface morphology of both MNB and Fe_3O_4 @fibroin-Pd was studied and imaged utilizing a scanning electron microscope (SEM) equipped with an

energy-dispersive X-ray (EDX) facility to investigate the chemical composition. A very thin layer of gold has covered the samples for both SEM and EDX analyses before imaging to prevent charging effects and to have enhanced electrical conductivity. The SEM images Fig. 1a, b transparently show that the MNB had a spherical formation with diameters of 16–20 nm. Figure 1c, d proves that no aggregation happened after treating with palladium acetate during the finishing step. EDX data also offer valuable information about the elements in the nano-biocomposite and the nanocatalyst. Figure 1e, f shows the EDX pattern of MNB and $\text{Fe}_3\text{O}_4@\text{fibroin-Pd}$, respectively. The peaks confirmed that the final nanocatalyst was composed of carbon (C) and nitrogen (N) indication of fibroin structure, iron (Fe) and oxygen (O) indication of Fe_3O_4 , and palladium (Pd) element.

TEM

Transmission electron microscopy (TEM) can provide more details about the internal structure and morphology of the prepared nanocomposite. As was previously observed in SEM images, in the TEM images the particles had also spherical morphology with diameters in the range of 16–20 nm for the MNB (Fig. 2). The images of the MNB are presented on different scales, and at the highest magnification, it can be better seen that the surface of nano-biocomposite is rather blurry due to the fibroin coating.

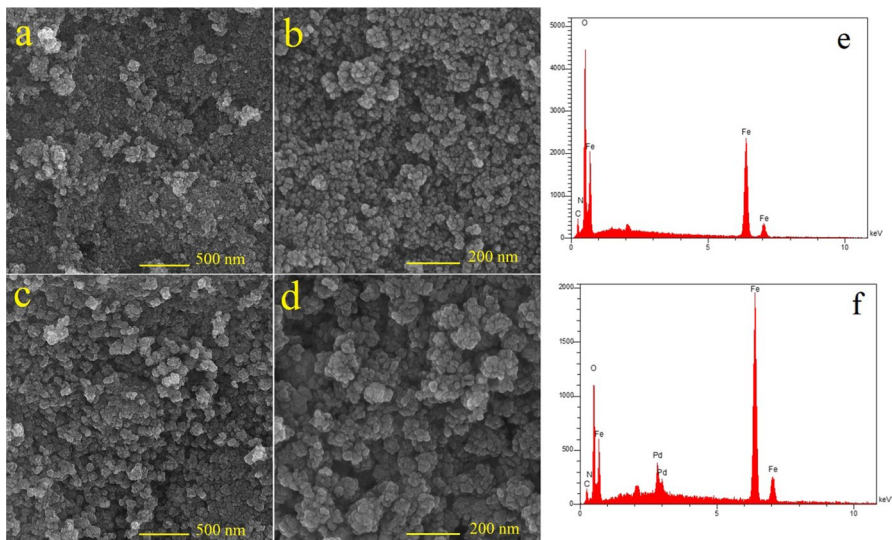


Fig. 1 SEM images of fibroin-based magnetic nano-biocomposite (MNB) (a and b), $\text{Fe}_3\text{O}_4@\text{fibroin-Pd}$ (c and d). EDX patterns of MNB (e) and $\text{Fe}_3\text{O}_4@\text{fibroin-Pd}$ (f)

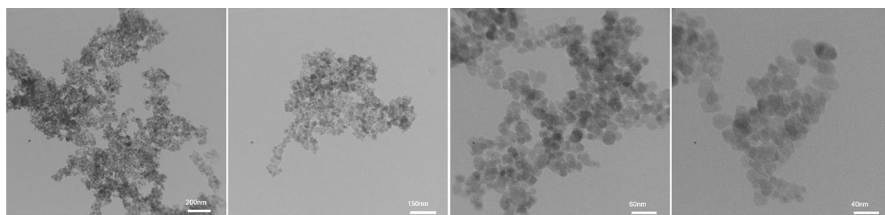


Fig. 2 TEM micrograph of MNB at different scales

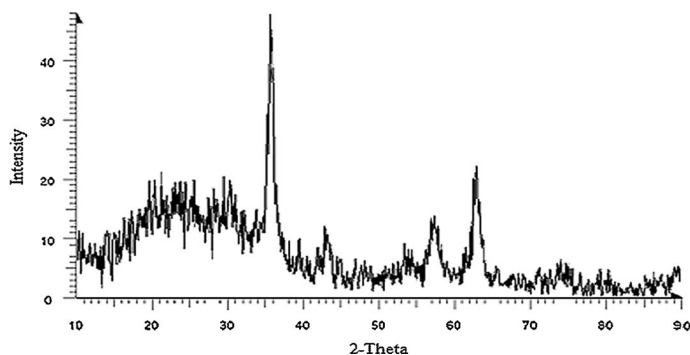


Fig. 3 XRD patterns of MNB

XRD

X-ray diffraction (XRD) patterns of MNB were measured by X-ray diffraction spectroscopy, and along with Fe_3O_4 , it is presented in Fig. 3. Six diffraction peaks appeared at $2\theta = 30.6^\circ$, 35.6° , 43.5° , 53.4° , 57.6° , and 63.4° corresponding to the (220), (311), (400), (422), (511), and (440) planes of pure Fe_3O_4 [33, 34].

TGA

Thermogravimetric analysis (TGA) of MNB is presented in Fig. 4. The TGA curve of MNB shows first weight loss below 120°C due to the removal of adsorbed water. The second weight loss happened in the range $220\text{--}411^\circ\text{C}$, indicating the decomposition of organic content (fibroin) presented in the sample. The thermal stability of the nano-biocomposite is up to 220°C , confirming that utilizing MNB is suitable as a stable support for catalyst systems at high temperatures.

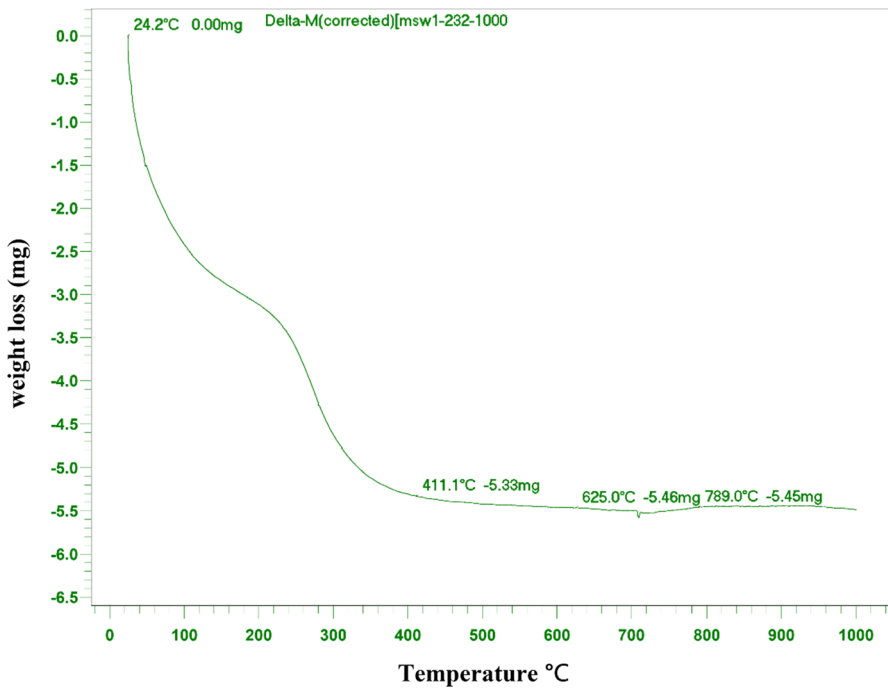


Fig. 4 Thermogravimetric analysis of fibroin magnetic nano-biocomposite (MNB)

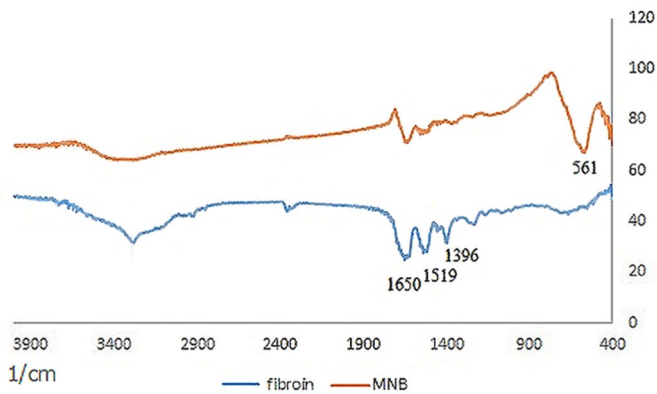


Fig. 5 FT-IR spectra of silk fibroin and MNB

FT-IR

FT-IR spectra of fibroin and MNB are shown in Fig. 5. In the fibroin spectrum (Fig. 5a), three distinct bands can be observed at 1650, 1519, 1396 cm^{-1} corresponding to primary, secondary, tertiary amide functional groups, respectively [35]. Figure 5b

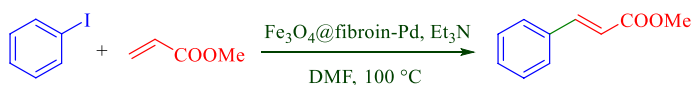
also shows MNB spectrum containing a new band at 561 cm^{-1} correspondings to Fe–O stretching vibration because of the presence of Fe_3O_4 nanoparticles in MNB [36].

ICP-OES analysis

Finally, the content of Pd immobilized on the surface of MNB was measured by inductively coupled plasma optical emission spectroscopy (ICP-OES) technique. The Pd loading content is 7.77 wt% revealed that the high loading of palladium was immobilized. The palladium loading shows the high performance of fibroin-based magnetic nano-biocomposite to keep metals.

Catalytic activity

The performance of the prepared nanocatalyst was examined in the C–C bond formation through Heck cross-coupling reaction (Scheme 2). The construction of the C–C bond is a fundamental reaction in organic synthesis and widely used in the synthesis of natural products, drugs, and polymeric materials [37]. The Heck cross-coupling



Scheme 2 Heck cross-coupling reaction of iodobenzene and methyl acrylate

reaction is one of the most important C–C forming reactions and has been studied to develop efficient catalysis protocols [38, 39]. Due to wide applications, C–C bond formation via Heck cross-coupling reaction was selected to investigate the catalytic performance of Fe_3O_4 @fibroin-Pd.

To determine the optimized reaction conditions, a series of experiments were carried out, and the reaction of iodobenzene and methyl acrylate was chosen as a model reaction (Table 1). Different reaction terms were changed, and it was found that 0.001 g of catalyst, $100\text{ }^\circ\text{C}$ temperature, and Et_3N as a base in DMF afforded the most desirable medium for this reaction (Table 1, entry 10).

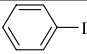

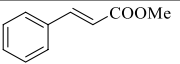
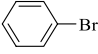

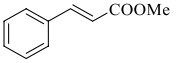
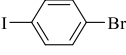

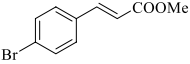
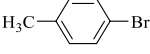

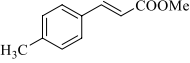
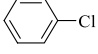

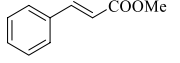
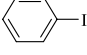
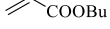
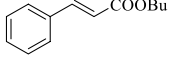
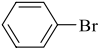

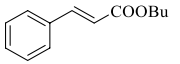
General method of the Heck coupling reaction

A round-bottomed flask equipped with a magnetic stirrer was filled with 0.5 mmol of aryl halide, 0.75 mmol of olefin, 1 mmol of Et_3N , 0.001 g of Fe_3O_4 @fibroin-Pd, and 1.5 mL of DMF. The reaction continued for an appropriate time under stirring at $100\text{ }^\circ\text{C}$. The progress of the reaction was assessed using thin-layer chromatography (TLC). Once the reaction was finished, the nanocatalyst was separated by an external magnet. The products were extracted with ethyl acetate, and then, the organic layer was washed with water and dried by MgSO_4 . The reaction was carried out with various aryl halides, and results are shown in Table 2. The structural features of products were characterized using spectral data IR, ^1H NMR, and ^{13}C NMR.

Table 1 Optimization of the reaction condition

Entry	Amount of catalyst ^a (g)	Base	Solvent	Temperature (°C)	Time (h:min) ^b	Yield (%) ^c
1	0.0007	Et ₃ N	H ₂ O	100	00:25	55
2	0.001	Et ₃ N	H ₂ O	100	00:12	75
3	0.0015	Et ₃ N	H ₂ O	100	00:15	75
4	0.003	Et ₃ N	H ₂ O	100	00:20	78
5	—	Et ₃ N	H ₂ O	100	24:00	-
6	0.001	KOH	H ₂ O	100	00:35	65
7	0.001	NaOH	H ₂ O	100	00:30	60
8	0.001	K ₃ PO ₄	H ₂ O	100	00:25	70
9	0.001	Et ₃ N	EtOH	100	00:25	70
10	0.001	Et ₃ N	DMF	100	00:09	96
11	0.001	Et ₃ N	DMSO	100	00:35	60
12	0.001	Et ₃ N	DMF	120	00:10	94
13	0.001	Et ₃ N	DMF	80	00:15	85
14	0.001	Et ₃ N	DMF	R.T	24:00	-

^aReaction was performed in the presence Fe₃O₄@fibroin-Pd^bDetected by TLC^cIsolated yield**Table 2** Heck coupling reactions of aryl halides with olefins^a

Entry	Aryl halide	Olefin	Product	Time (h:min) ^b	Yield (%) ^c
1				00:09	96
2				00:12	92
3				00:05	92
4				00:20	87
5				00:35	45
6				00:15	94
7				00:20	85

^a Reaction condition: aryl halide (0.5 mmol), olefin (0.75 mmol), Et₃N (1 mmol), catalyst (0.001 g), DMF (1.5 mL), at 100 °C.^b Detected by TLC.^c Isolated yield.

Table 3 Comparison of Fe_3O_4 @fibroin-Pd results in the Heck coupling reaction with similar researches

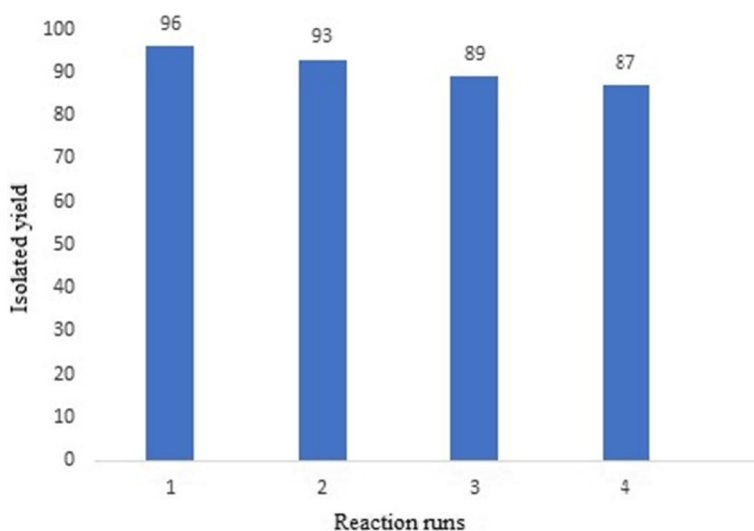
Entry	Catalyst	Solvent	Temperature (°C)	Time (h:min)	Yield (%)	Ref
1	CMC-Pd ^{II}	DMF	110	03:00	85	[40]
2	Pd/ Fe_3O_4 @PIL-NH ₂	Solvent-free	125	00:25	94	[41]
3	Pd@OMP-DVB	DMF	80	00:30	99	[42]
4	Pd-NPs/P.a.kurdica gum	H ₂ O	80	00:25	98	[43]
5	Fe_3O_4 /DAG/Pd	DMF	110	01:00	90	[44]
6	Fe_3O_4 @fibroin-Pd	DMF	100	00:09	96	This work

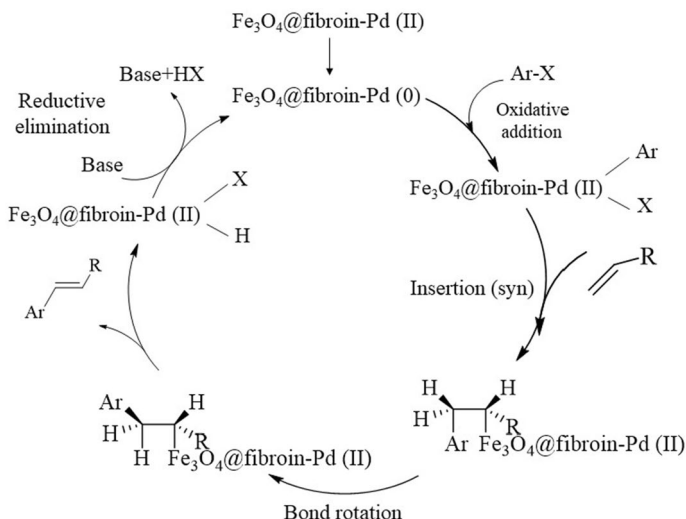
Comparison of Fe_3O_4 @fibroin-Pd results with some similar works

A direct comparison of Fe_3O_4 @fibroin-Pd and recently reported papers in the Heck coupling reaction proves the strong performance of the nanocatalyst (Table 3).

Catalyst recyclability

In the ensuing lines, the recyclability of Fe_3O_4 @fibroin-Pd is assessing. The yield of the model reaction catalyzed by untouched Fe_3O_4 @fibroin-Pd was compared with the yields obtained by recovered Fe_3O_4 @fibroin-Pd. After completion of the first round Heck coupling reaction, the nanocatalyst was separated by an external magnet and washed with water and ethanol followed by drying at 100 °C overnight. This recycling process was performed up to four reactions round, and the yields are presented in Fig. 6. The results proved that Fe_3O_4 @fibroin-Pd could be employed for four consecutive reaction runs without a considerable decrease in activity.

**Fig. 6** Reusability of the Fe_3O_4 @fibroin-Pd



Scheme 3 Proposed mechanism for the Heck cross-coupling reaction in the presence of $\text{Fe}_3\text{O}_4@\text{fibroin-Pd}$

Leaching

In supported metal catalysts, including palladium, leaching is a major problem that leads to loss of active sites in the nanocatalyst. To investigate whether or not the attachment of palladium on the fibroin surface is strong enough, the reaction between iodobenzene and methyl acrylate was again performed under optimal conditions. After half of the reaction time, the nanocatalyst was separated using an external magnetic field. The reaction was continued for 2 h under the same conditions without adding any fresh nanocatalyst. The reaction progress was monitored by TLC, and it showed that the coupling reaction no longer performed. Above results revealed that the palladium leaching phenomenon was insignificant in the Heck reaction, demonstrating the palladium deposited on magnetic nano-biocomposite $\text{Fe}_3\text{O}_4@\text{fibroin}$ acts as a heterogeneous catalyst in the reaction. A plausible mechanism for the Heck reaction, based on previous reports [45], is proposed in Scheme 3.

Conclusion

Herein, we demonstrated a successful preparation of $\text{Fe}_3\text{O}_4@\text{fibroin-Pd}$ by employing a simple, economical, and eco-friendly strategy for the Heck coupling reaction. The prepared nanocatalyst possessed high surface areas, excellent thermal stability, easy separation ability, uniform morphology, and high catalytic activity. The core-shell structure of $\text{Fe}_3\text{O}_4@\text{fibroin}$ was the main reason for the high functionalization capacity of fibroin as a support for metal. Thus, the successful example opens up a new avenue in constructing new core-shell type magnetic nanocatalysts with good catalytic performance and leads to preparation of other metal functional catalysts with special requirements for organic reactions.

Supplementary Information The online version contains supplementary material available at <https://doi.org/10.1007/s11164-021-04462-2>.

Acknowledgements The authors acknowledge the financial support from the Semnan University Research Council.

References

1. M. Govindappa, S. Tejashree, V. Thanuja, B. Hemashekhar, C. Srinivas, O. Nasif, A. Pugazhendhi, V.B. Raghavendra, *J. Drug Deliv. Sci. Technol.* **61**, 102289 (2021)
2. U. Munawer, V.B. Raghavendra, S. Ningaraju, K.L. Krishna, A.R. Ghosh, G. Melappa, A. Pugazhendhi, *Int. J. Pharm.* **588**, 119729 (2020)
3. S. Ningaraju, U. Munawer, V.B. Raghavendra, K.S. Balaji, G. Melappa, K. Brindhadevi, A. Pugazhendhi, *Anal. Biochem.* **612**, 113970 (2021)
4. A. George, P.A. Shah, P.S. Shrivastav, *Int. J. Pharm.* **561**, 244–264 (2019)
5. H. Yang, B. Jia, Z. Zhang, X. Qu, G. Li, W. Lin, D. Zhu, K. Dai, Y. Zheng, *Nat. Commun.* **11**, 1 (2020)
6. M. Aldas, C. Pavon, H. De La Rosa-Ramírez, J.M. Ferri, D. Bertomeu, M.D. Samper, J. López-Martínez, *J. Polym. Environ.* **20**, 1–15 (2021)
7. K.K. Sadasivuni, J.J. Cabibihan, D. Ponnammam, M.A. AlMaadeed, J. Kim, (Eds.). *Biopolymer Composites in Electronics*, (Elsevier, 2016)
8. N. Prakashkumar, M. Vignesh, K. Brindhadevi, N.-T. Phuong, *Prog. Org. Coat.* **151**, 106098 (2021)
9. A. Chrzanowska, A. Derylo-Marczewska, *Int. J. Biol. Macromol.* **139**, 531–542 (2019)
10. P. Makvandi, Z. Baghbantargarhdari, W. Zhou, Y. Zhang, R. Manchanda, T. Agarwal, A. Wu, T.K. Maiti, R.S. Varma, B.R. Smith, *Biotechnol. Adv.* **11**, 107711 (2021)
11. S. Shanmugam, S. Krishnaswamy, R. Chandrababu, U. Veerabagu, A. Pugazhendhi, T. Mathimani, *Fuel* **273**, 117777 (2020)
12. M. Kempasiddaiah, V. Kandathil, R.B. Dateer, M. Baidya, S.A. Patil, S.A. Patil, *J. Environ. Sci.* **101**, 189–204 (2021)
13. T. Bhengo, M. Moyo, M. Shumba, O. Okonkwo, *New. J. Chem.* **42**, 7 (2018)
14. R.K. Sharma, S. Dutta, S. Sharma, R. Zboril, R.S. Varma, M.B. Gawande, *Green Chem.* **18**, 11 (2016)
15. P. Naserzadeh, S.A. Mortazavi, K. Ashtari, A. Salimi, M. Farokhi, J. Pourahmad, *J. Biochem. Mol. Toxicol.* **32**, 6 (2018)
16. P. Akbarzadeh, N. Koukabi, *Appl. Organomet. Chem.* **34**, 3 (2020)
17. X. Xing, G. Cheng, C. Yin, X. Cheng, Y. Cheng, Y. Ni, X. Zhou, H. Deng, Z. Li, *Arab. J. Chem.* **13**, 5 (2020)
18. L. Giovannelli, A. Milanesi, E. Ugazio, L. Fracchia, L. Segale, *Pharmaceuticals* **14**, 3 (2021)
19. M. Ribeiro, M.P. Ferraz, F.J. Monteiro, M.H. Fernandes, M.M. Beppu, D. Mantione and H. Sardon. *Nanomedicine* **13**, 1 (2017)
20. M.A. Tomeh, R. Hadianamrei, X. Zhao, *Pharmaceutics* **11**, 10 (2019)
21. O. Bayraktar, F. Özyıldız, *Ozone: Sci. Eng.* **41**, 1 (2019)
22. Y. Han, S. Yu, L. Liu, S. Zhao, T. Yang, Y. Yang, Y. Fang, S. Lv, *Mol. Catal.* **457**, 24–32 (2018)
23. J. Liu, Z. Ding, G. Lu, J. Wang, L. Wang, Q. Lu, *Macromol. Biosci.* **19**, 12 (2019)
24. Q. Wang, G. Han, S. Yan, Q. Zhang, *Materials* **12**, 3 (2019)
25. T. Ikawa, H. Sajiki, K. Hirota, *Tetrahedron* **61**, 8 (2005)
26. B.B. Pekşen, C. Üzelakçıl, A. Güneş, Ö. Malay, O. Bayraktar, *J. Chem. Technol. Biotechnol.* **81**, 7 (2006)
27. Y. Xia, J. Wan, Q. Gu, *Gold. Bull.* **44**, 3 (2011)
28. P. Akbarzadeh, N. Koukabi, E. Kolvari, *Res. Chem. Intermed.* **45**, 3 (2019)
29. P. Akbarzadeh, N. Koukabi, E. Kolvari, *Mol. Divers.* **45**, 1009–1024 (2019)
30. S. Suzuki, A.M. Shadforth, S. McLenachan, D. Zhang, S.-C. Chen, J. Walshe, G.E. Lidgerwood, A. Pébay, T.V. Chirila, F.K. Chen, *Mater. Sci. Eng. C.* **105**, 110131 (2019)
31. R.R. Mallepally, M.A. Marin, M.A. McHugh, *Acta Biomater.* **10**, 10 (2014)
32. A.N. Parouch, N. Koukabi, E. Abdous, *Res. Chem. Intermed.* **46**, 7 (2020)

33. S. Lotfi, H. Veisi, *Mater. Sci. Eng. C* **105**, 110112 (2019)
34. X. Zhu, D. Hou, H. Tao, M. Li, J. *Alloys Compd.* **821**, 153580 (2020)
35. H. Hong, O.J. Lee, Y.J. Lee, J.S. Lee, O. Ajiteru, H. Lee, Y.J. Suh, M.T. Sultan, S.H. Kim, C.H. Park, *Biomolecules* **11**, 1 (2021)
36. M.K. Seliem, M. Barczak, I. Anastopoulos, D.A. Giannakoudakis, *Nanomater.* **10**, 4 (2020)
37. R. Narayana, *Molecules* **15**, 4 (2010)
38. F. Christoffel, T.R. Ward, *Catal. Lett.* **148**, 2 (2018)
39. Y. Bao, L. Shao, G. Xing, C. Qi, *Int. J. Biol. Macromol.* **130**, 203–212 (2019)
40. J. Xiao, Z. Lu, Y. Li, *Ind. Eng. Chem. Res.* **54**, 3 (2015)
41. W. Liu, D. Wang, Y. Duan, Y. Zhang, F. Bian, *Tetrahedron Lett.* **56**, 14 (2015)
42. B. Karimi, M.R. Marefat, M. Hasannia, P.F. Akhavan, F. Mansouri, Z. Artelli, F. Mohammadi, H. Vali, *ChemCatChem* **8**, 15 (2016)
43. H. Veisi, A.R. Faraji, S. Hemmati, A. Gil, *Appl. Organomet. Chem.* **29**, 8 (2015)
44. H. Veisi, A. Sedrpoushan, S. Hemmati, *Appl. Organomet. Chem.* **29**, 12 (2015)
45. R. Ma, P. Yang, F. Bian, *New. J. Chem.* **42**, 6 (2018)

Publisher's Note Springer Nature remains neutral with regard to jurisdictional claims in published maps and institutional affiliations.